Realistic Covariance Generation for the GPM Spacecraft

Siamak G. Hesar and Matthew Duncan
SpaceNav, Boulder, CO 80301

James H. Pawloski
NASA Goddard Space Flight Center, Greenbelt, MD 20771

Prepared for SpaceOps 2018
June 1, 2018

Introduction

- Global Precipitation Measurement (GPM) mission is an international effort for collecting worldwide observations of rain and snow.
- It was launched on February 27, 2014 by NASA and the Japanese Aerospace Exploration Agency (JAXA)
- GPM Core Observatory Satellite Orbit:
  - Circular non-Sun-synchronous orbit
  - 65 degrees inclination
  - ~400 km altitude
- Currently GPM is below the International Space Station (ISS).
- On orbit collision risk:
  - Cataloged debris objects
  - Occasional smallsat/cubesat objects deployed from the ISS.
- Both operational scenarios require an accurate knowledge of the expected GPM prediction errors as a function of time.
- The challenge is to represent the proper (realistic) distribution of the satellite state in a future time.

Visualization of the GPM Core Observatory and partner satellites.
Credits: NASA

SPACENAV

Introduction

- Many times, the state uncertainty reported by the orbit determination (OD) process tends to underrepresent the true level of uncertainty in the state solution.
- Furthermore, simplifying Gaussian assumption for the distribution of the predicted satellite states may not hold after long propagation durations.
- Other methods when Gaussian assumption isn't valid
  - Gaussian Mixture Models
  - Gauss von Mises model
  - Polynomial chaos
- Operationally, however, the conventional method based on the joint Gaussian distribution of the primary and secondary objects is used for the computation of the collision probability at the time of closest approach.
  - Collision probability reported by the Joint Space Operations Center (JSpOC)
- Hence, it is very important to confirm that the predicted covariance generated and delivered to JSpOC for screening is both realistic and also does not violate the Gaussian assumption.
- SpaceNav Covariance Realism Tool (CRT), accomplishes this by inflating the propagated covariance via a set of tuned process noise parameters.
- Goodness-of-Fit (GOF) test is then performed to test for the Gaussian assumption of the predicted error population and the propagated uncertainties.

SPACENAV

An Overview of the GPM Covariance Realism Process

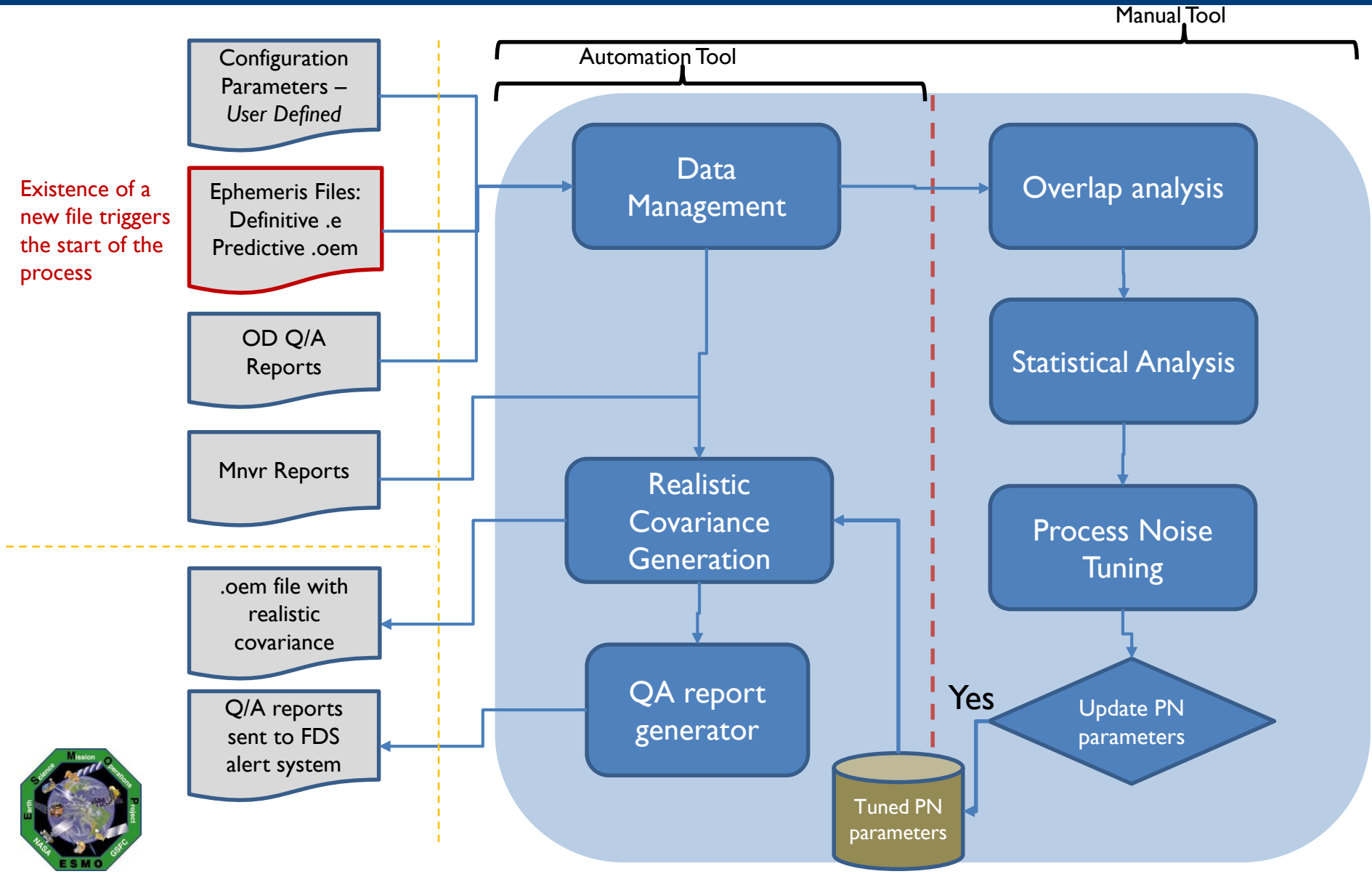

Statistical Analysis & Overlap Comparison

- The goal of the overlap analysis is to provide a measure of the accuracy of the predictive ephemerides and a realistic characterization of the expected propagation errors.
- This method performs a comparison between the ***definitive*** and the ***predictive*** states over several epochs.
- The divergence of predictive ephemerides from the definitive ones is used to empirically represent the expected level of error growth in the propagated state.
- Due to inherent errors in the definitive ephemeris, this method really shows the ***relative*** error growth between the OD solution and the predicted trajectory.

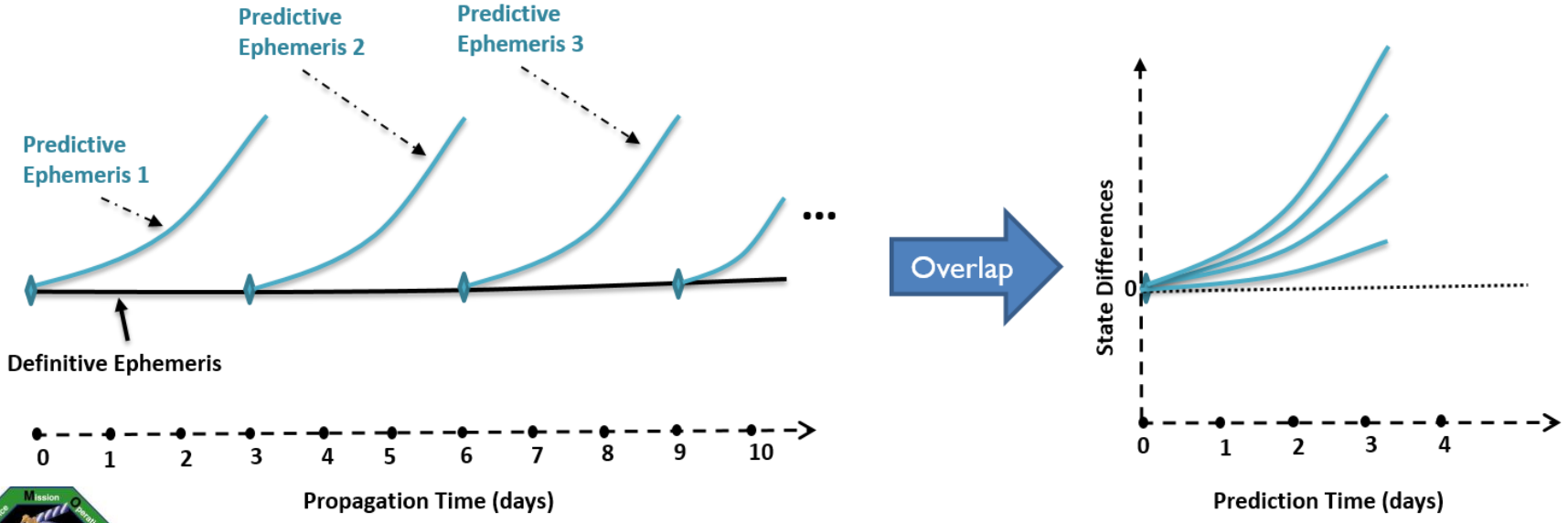

SPACENAV

Statistical Analysis & Overlap Comparison
Outlier Removal

- Some of the predicted ephemeris files contain predicted maneuvers.
- Errors in the predicted maneuvers vs. what was actually executed (definitive ephem) result in large predicted state errors that need to be removed from overlap statistics.
- Maneuver uncertainty may be added later at the time of realistic covariance generation.
- We consider overlap data from January 2016 till March 2018.
- We consider every other 3 predicted file to make sure that the overlapped state differences are independent.

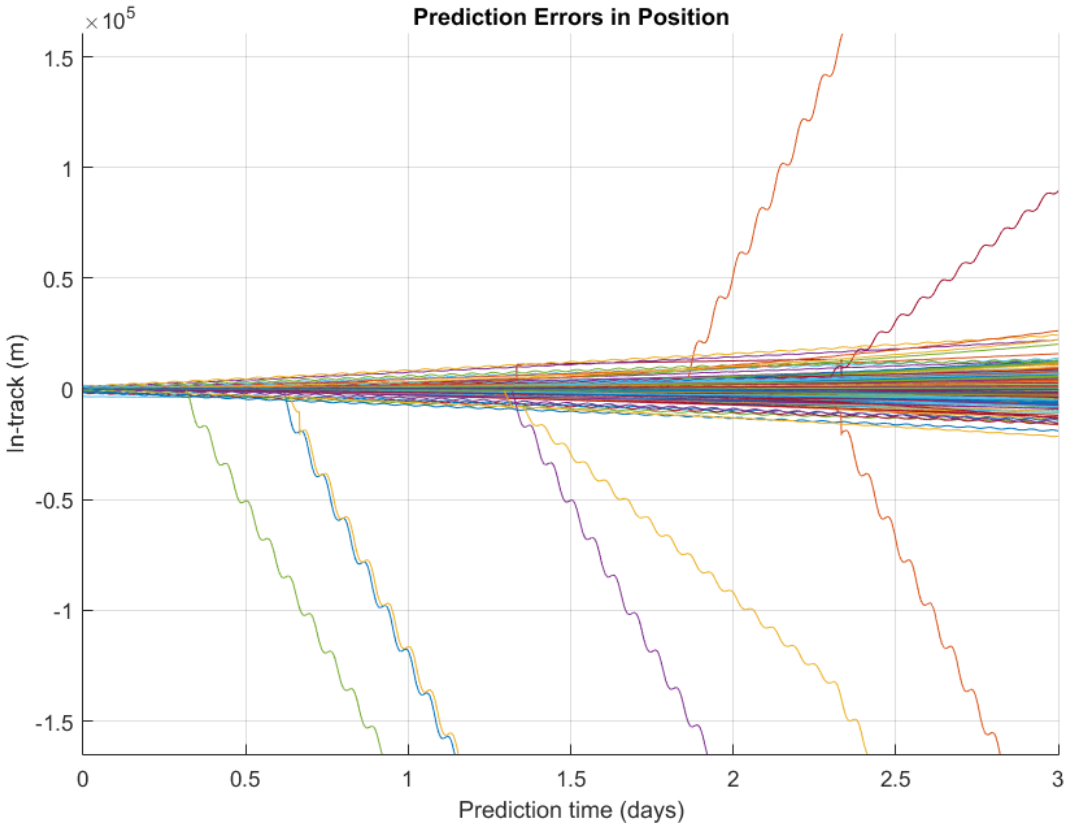

SPACENAV

Statistical Analysis & Overlap Comparison
Outlier Removal

- A Recursive sigma level outlier removal scheme is used. The recursion ends when no more outlier is identified.
- Overlap state differences after outlier removal is performed.
- Majority of the state differences are within $\pm 3\sigma$ (Standard Deviation) of the data.
- State differences are smooth and well-behaved.
- A total of 232 trajectories remain after outlier removal is completed.

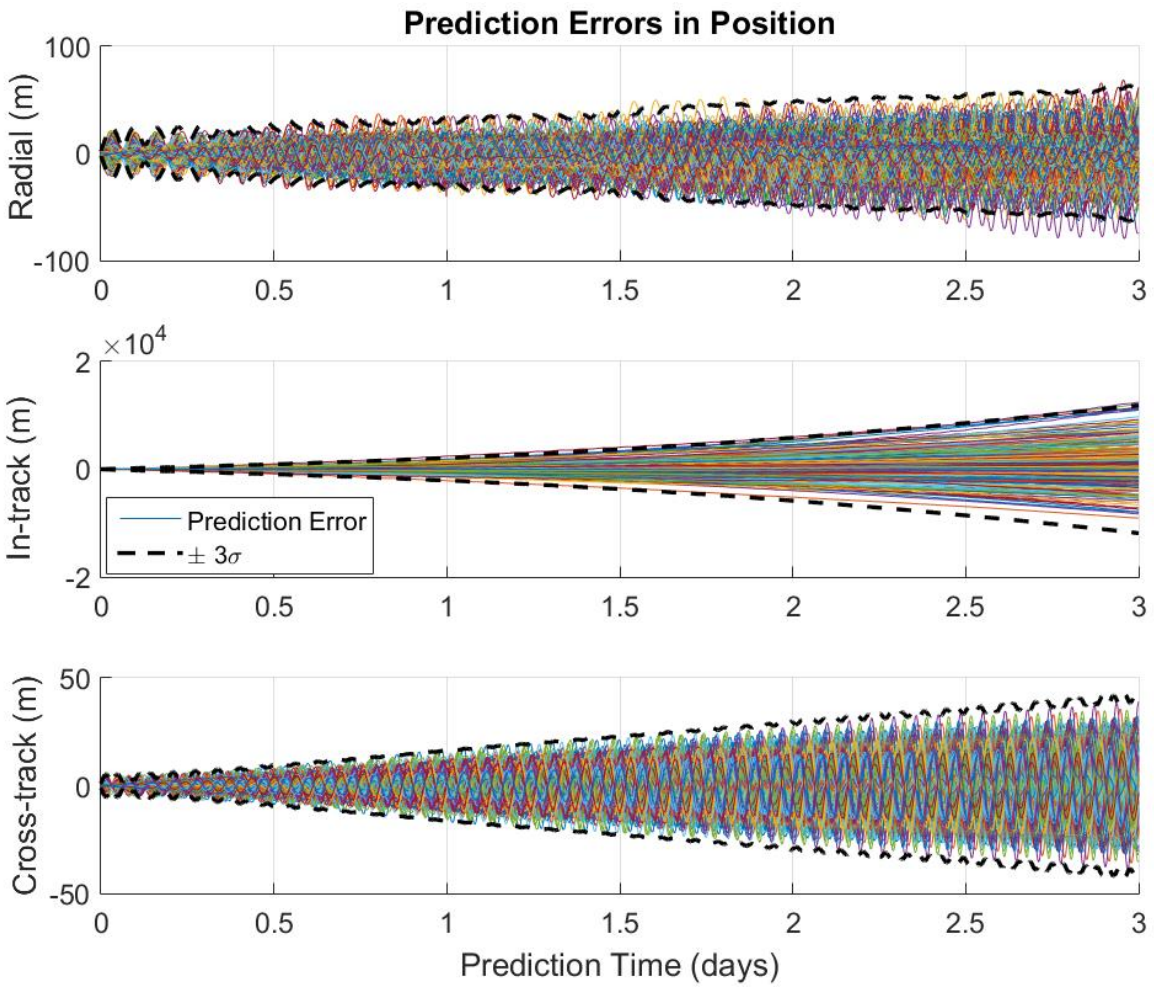

SPACENAV

Statistical Analysis & Overlap Comparison vs. FOT Prediction

- The overlapped predicted errors vs. the predicted uncertainty for a handful of selected ephemeris generated by GPM flight operation team (FOT).
- The curves generated by different FOT files look as if they fall on top of each other at the scale of this plot.
- The predicted uncertainty generated by the FOT underestimates the observed level of dispersion that exists in the predicted errors.
- That is, FOT predicted uncertainty is not a realistic representation of the actual prediction error dispersion.

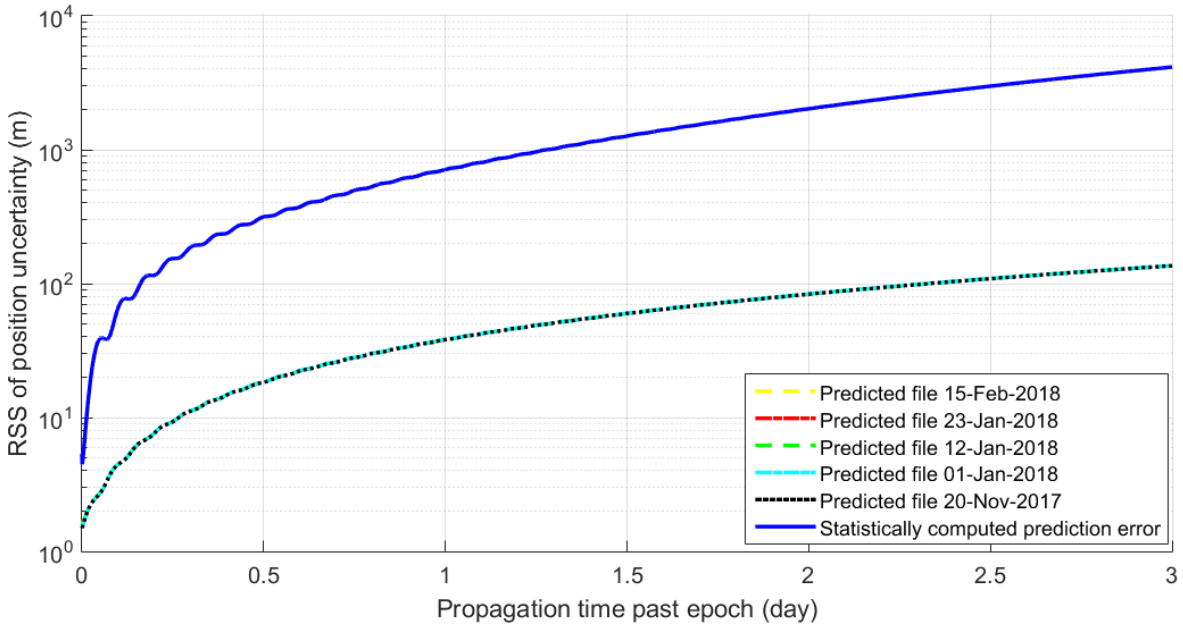

SPACENAV

Statistical Analysis of the Overlapped Data
Test for Gaussian Assumption

- Mahalanobis distance
  - $d^2 = \delta \boldsymbol{X}^T \bar{P}^{-1} \delta \boldsymbol{X}$

  where

  $\delta \boldsymbol{X}_{3\times 1}$: Predictive position error

  $\bar{P}$: Covariance given by the data or predictive covariance
- $d^2 \sim \chi^2(3)$ *iff* $\delta \boldsymbol{X} \sim N(0, \bar{P})$
- *p-values* corresponding to 3-DoF χ^2 GOF test for the ***prediction position errors alone***.
- The results show one can safely assume that the predicted errors (after the outlier removal) follow a Gaussian distribution.

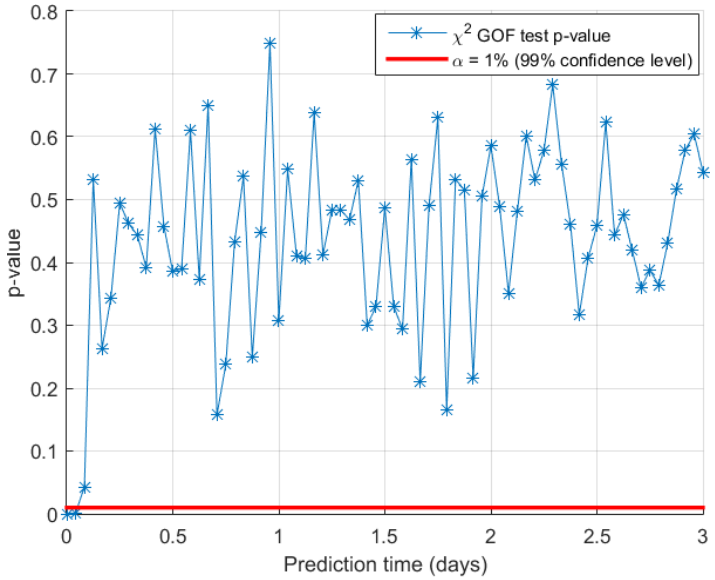

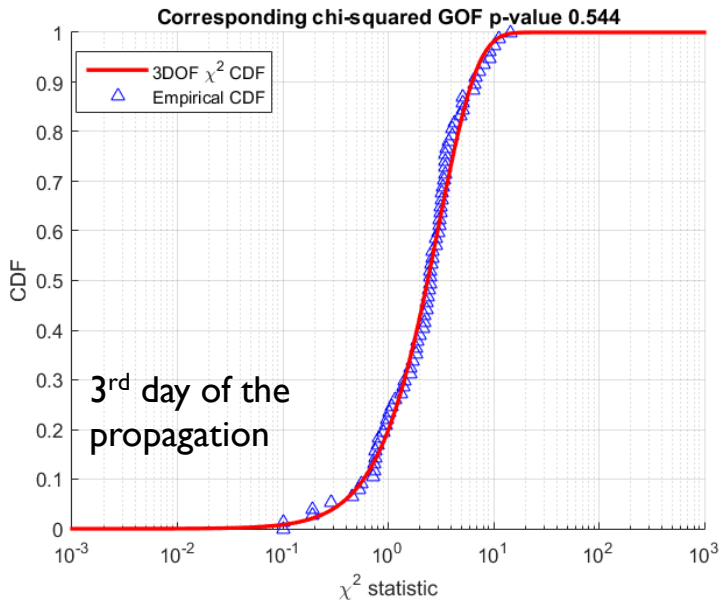

Statistical Analysis of the Overlapped Data
Test for Gaussian Assumption

- Scatter plot of the position error population.
- Radial, In-track, and X-track standard errors.
- Uncertainty ellipses are computed from the data pool.

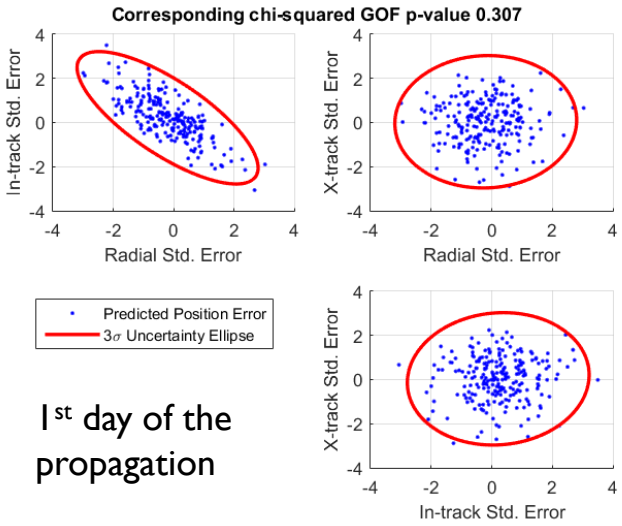

1st day of the propagation

Strong correlation between radial and in-track components.

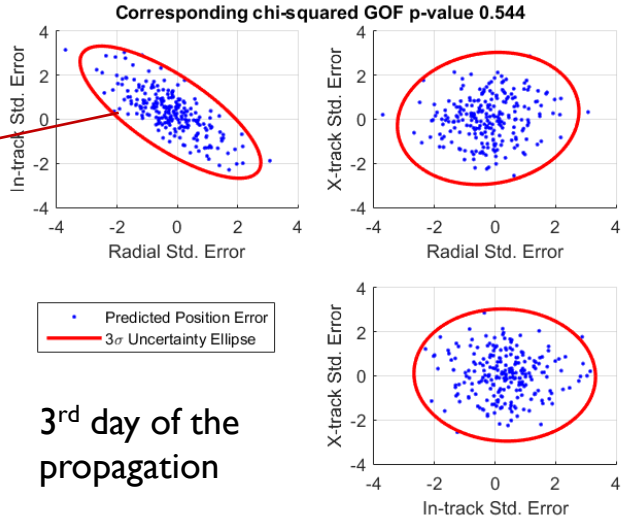

3rd day of the propagation

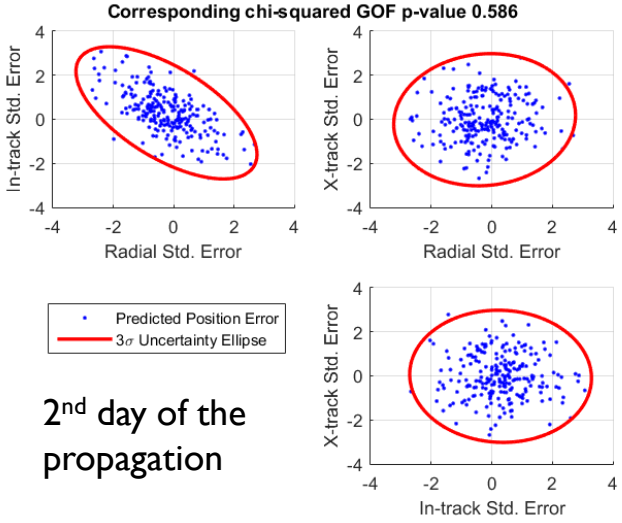

2nd day of the propagation

SPACENAV

Statistical Analysis of the Overlapped Data
Test for Gaussian Assumption

- What if the prediction errors are scaled by the FOT provided covariance?
- The FOT predicted uncertainty pushes the data away from the Gaussian distribution.
- FOT provided uncertainty is NOT realistic.

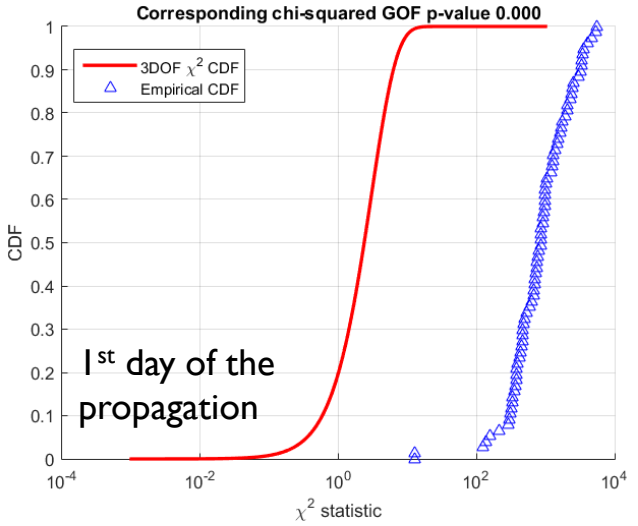

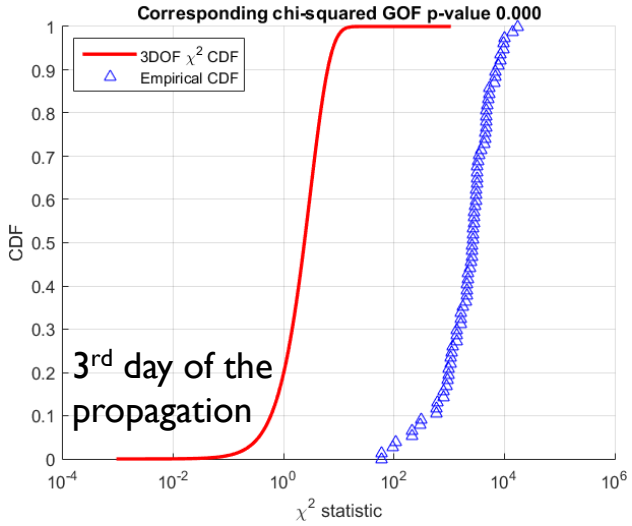

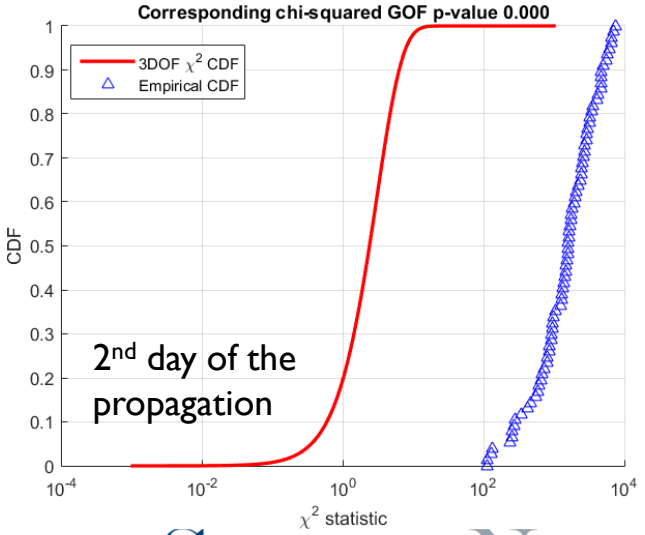

SPACENAV

Process Noise Tuning
Formulation

- Process noise is a way for the dynamical model to compensate for unknown or mismodeled accelerations present in that model.
- The process noise is implemented by including stochastic accelerations into the predicted covariance propagated forward in time.
- This is done by augmenting the linear mapping of the covariance matrix with and additional inflation term:

$$P_{k+1} = \Phi_{k+1,k}\, P_k \Phi_{k+1,k}^T + \Gamma_{k+1,k} Q_k \Gamma_{k+1,k}^T$$

- The process noise transition matrix, Γ, is used to map Q forward in time.
- The process noise matrix, *Q*, is composed of acceleration terms in the radial, in-track, and cross-track directions

$$Q = \begin{bmatrix} \sigma_{a_R}^2 & 0 & 0 \\ 0 & \sigma_{a_I}^2 & 0 \\ 0 & 0 & \sigma_{a_C}^2 \end{bmatrix}$$

- The process noise terms are accelerations, hence in one dimensional case is simplifies to

$$\sigma_{k+1} = \Phi_{k+1,k}\sigma_k + \frac{1}{2}(\Delta t)^2 \sigma_a$$

SPACENAV

Process Noise Tuning
Metrics

- "Tuning" of process noise parameters means that we select a set of parameters that minimize a certain cost function.
- In this case, the cost function is the difference between the statistically derived prediction error profile and the propagated uncertainty.
- There are many ways for defining the cost function (metric) of the difference between the two uncertainty profiles.
- Two metrics are considered for this analysis:
  - Mean percent difference along the propagated arc – Err_mean
  - Final difference percentage (averaged over one orbit period rather than a single point) – Err_final
- Following analysis compares these two metrics.
- An iterative least squares targeting method was used to perform the tuning.

SPACENAV

Process Noise Tuning
Metrics – GOF tests

- The process noise tuning was performed for all of the predicted trajectories.
- The parameters were tuned against the to different metrics for **3-day** prediction period.
- New covariance profile was generated based on each tuned process noise parameter set.
- The χ^2 statistic was computed for each prediction time based on the new propagated covariance.
- The GOF test *p-value* plot shows that the addition of the process noise generates realistic covariance for more that ~50% of the propagation times.
- The location of the best fit is a function of the tuning metric; mean vs. final error.

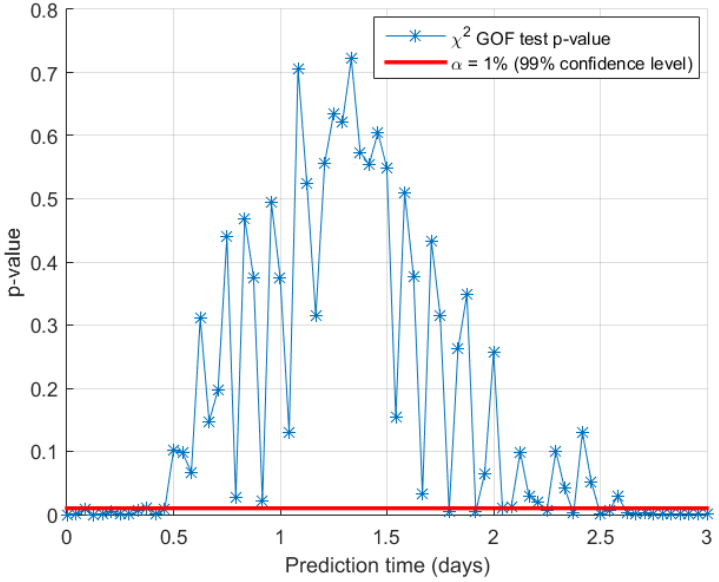

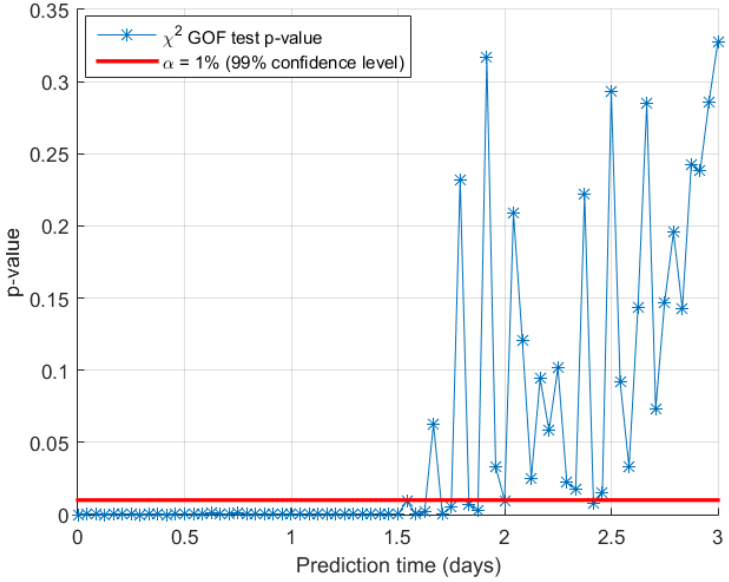

Process Noise Tuning
Metrics – GOF tests

- Tuning to the final error at 3 days of prediction.
- Close agreement between the empirical cumulative distribution function (ECDF) derived from the data and the hypothesized distribution after 3 days of propagation.
- There is also a good visual agreement between the two curves after 1 day and 2 days of propagation, even though the p-value suggests otherwise.
- The large number of the test population results in a very strict statistical GOF test which is sensitive to small amounts of deviations from the hypothesized distribution.

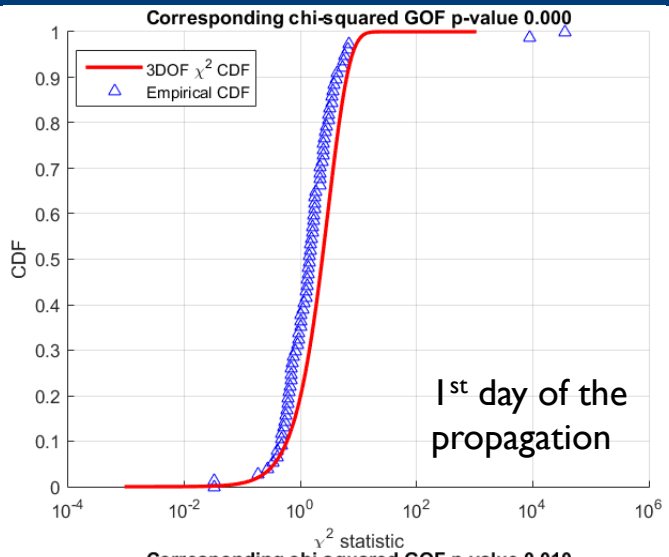

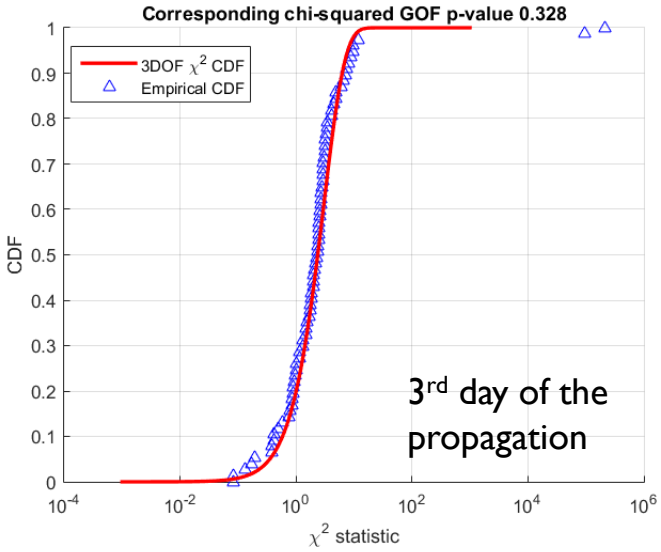

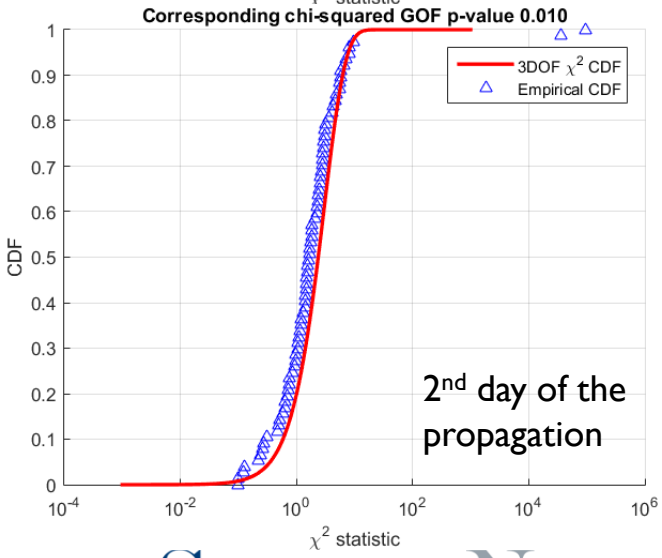

SPACE NAV

Process Noise Tuning
Sensitivity Analysis

- It is also of interest to look at the effect of tuning to different prediction time spans, as one may need the tuning done for a shorter than 3 day time span during an operational scenario.
- This plot shows the tuned process noise parameters to the ***final percent*** difference metric, and to 1, 2, and 3 day time spans.
- The results show that the in-track and cross-track process noise parameters increase as the tuning span is increased.
- Interestingly, the radial portion decreases. This may be un-intuitive at first, however, the reason for the decreasing radial PN parameters is the increasing in-track parameters that more than compensate for the radial portion via their correlation.

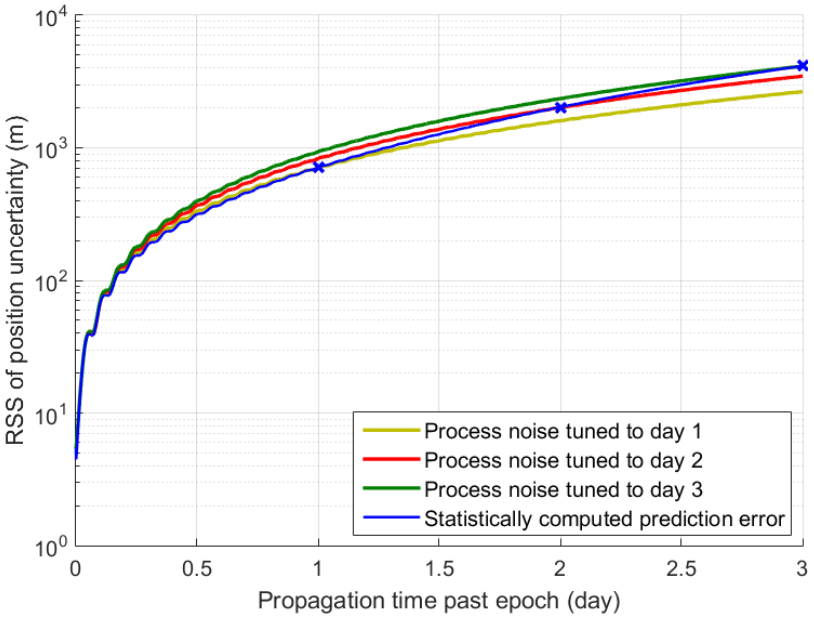

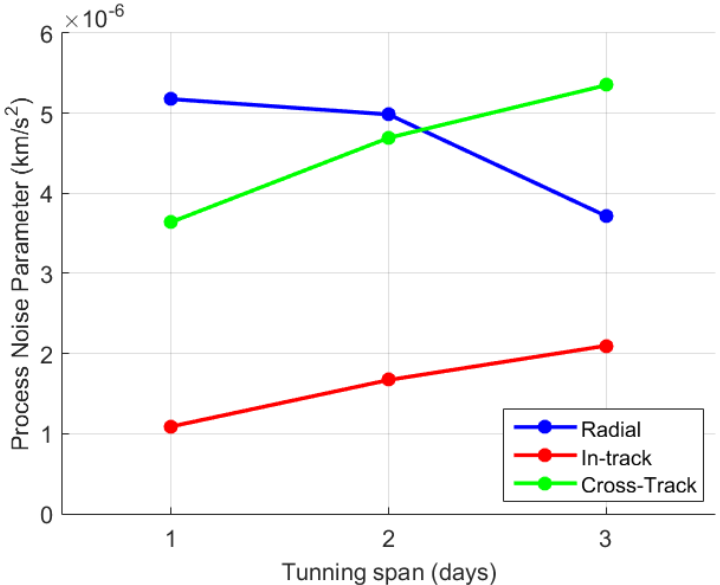

Maneuver Uncertainty Implementation
Methodology

- GPM spacecraft executes maneuvers frequently during its normal operations.
- Errors in maneuver execution will lead to errors in the propagated state of the spacecraft.
- Depending on the size of the maneuver and the error level, maneuver execution results in an increased propagated state uncertainty.
- *Gates Model* for maneuver execution error
  - Maneuver Magnitude Error
    - Bias in the maneuver magnitude, ϵ_1
    - Proportional error, ϵ_2
  - Pointing Error
    - Bias in pointing, ϵ_3
    - Proportional error in pointing, ϵ_4
  - $\delta\Delta\boldsymbol{V} = \sqrt{\epsilon_1^2 + |\Delta\boldsymbol{V}|^2\epsilon_2^2}\,\hat{\boldsymbol{e}}_1 + \sqrt{\epsilon_3^2 + |\Delta\boldsymbol{V}|^2\epsilon_4^2}\,\hat{\boldsymbol{e}}_2 + \sqrt{\epsilon_3^2 + |\Delta\boldsymbol{V}|^2\epsilon_4^2}\,\hat{\boldsymbol{e}}_3$
  - $\hat{\boldsymbol{e}}_1, \hat{\boldsymbol{e}}_2, \hat{\boldsymbol{e}}_3$ are the basis vectors of the maneuver coordinate frame such that $\hat{\boldsymbol{e}}_1$ is aligned with $\Delta\boldsymbol{V}$ direction.

Maneuver Uncertainty Implementation
Analysis of the Past Performance

- Maneuver type breakdown since the s/c launch:
  - A total of 22 type 1 maneuvers (fwd facing – prograde) – thrusters 1 – 8
  - A total of 27 type 2 maneuvers (bwd facing – prograde) – thrusters 9 – 12
  - 2 type 3 maneuvers (bwd facing – retrograde) – thrusters 1 – 8
  - One type 4 maneuver (fwd facing – retrograde) – thrusters 9 – 12
- With only a few retrograde maneuvers one can not establish statistically significant results, hence
- In analyzing the statistical performance of maneuvers, we consider maneuvers that use the same thruster set as the same type, i.e.

Maneuver Type	S/C yaw orientation (deg)	Thruster set	Resulting Maneuver
1	0 – forward facing	aft (thrusters1 – 8)	Prograde
2	180 – backward facing	fwd (thrusters 9 – 12)	Prograde
1	180 – backward facing	aft (thrusters1 – 8)	Retrograde
2	0 – forward facing	fwd (thrusters 9 – 12)	Retrograde

SPACENAV

Maneuver Uncertainty Implementation
Analysis of the Past Performance

- Maneuver execution error history – ***Percent errors***
- There is not a strong visible correlation between the maneuver magnitude and relative error scale.
- The same outliers also exist in the absolute error scale.

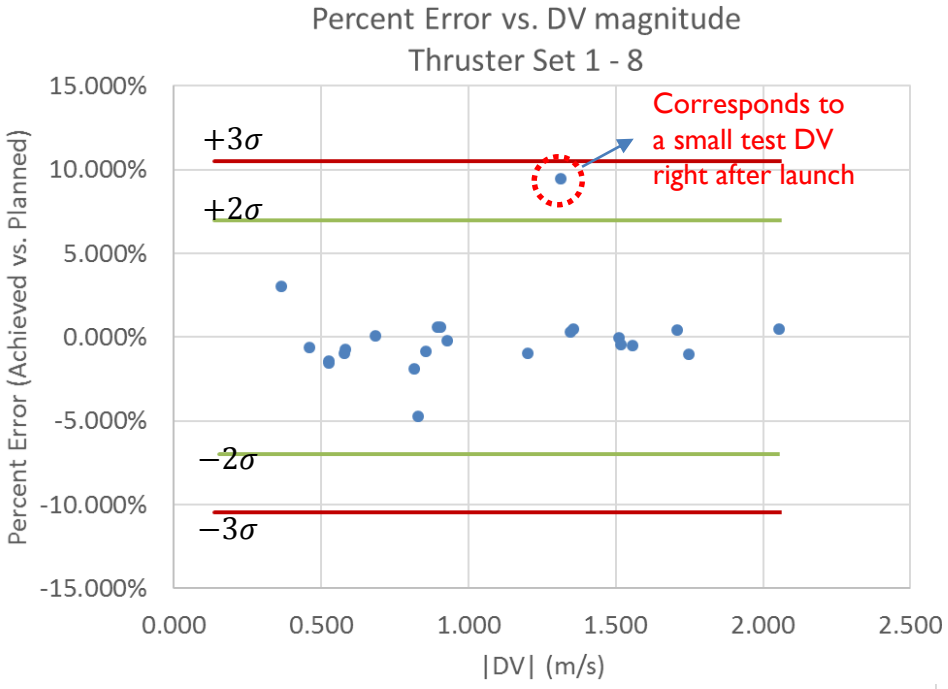

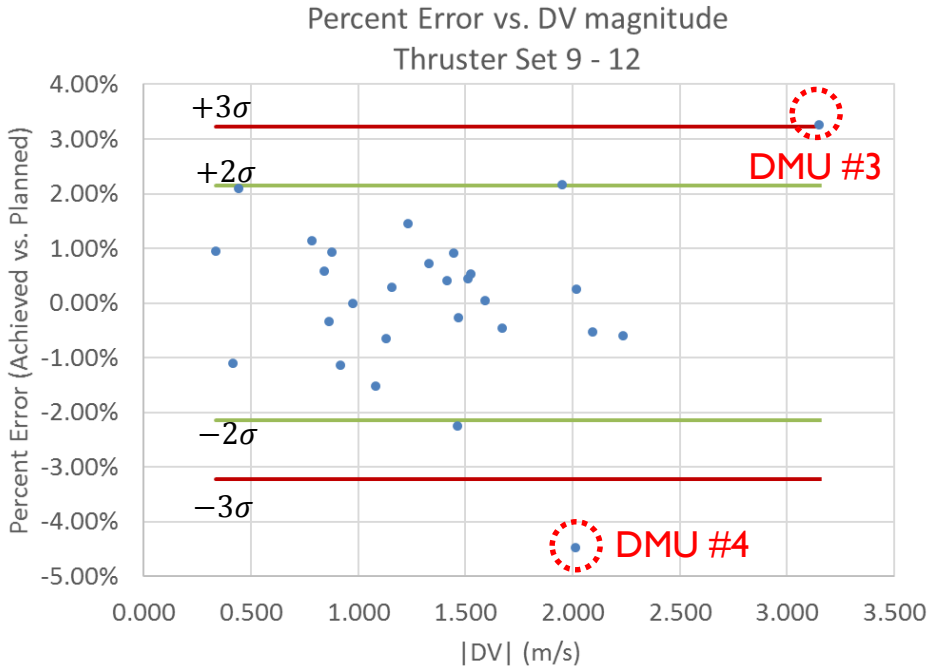

SPACE NAV

Maneuver Uncertainty Implementation
Analysis of the Past Performance

- At last, based on the analysis of the available data on the performance of the thrusters thus far, we arrive at the following performance values for two types of maneuvers.
- The values are computed after taking out the outliers
- We take the root mean square (RMS) of the residuals as the 1-sigma uncertainty level for the maneuvers, per maneuver type.
- Pointing errors are assumed to be negligible.

Maneuver Type	# of Data Points	Mean (m/s)	Standard Deviation (m/s)	RMS (m/s)
1 - aft (thrusters1 – 8)	23	0.002	0.029	0.028
2 - fwd (thrusters 9 – 12)	26	0.001	0.014	0.013
Relative Errors				
1 - aft (thrusters1 – 8)			2.48%	2.43%
2 - fwd (thrusters 9 – 12)			1.07%	1.05%

SPACENAV

Maneuver Uncertainty Implementation
Example

- Maneuver execution errors are considered in the realistic covariance generation tool.
- Example:
  - Magnitude: 0.459 m/s
  - Time: 09/15/17 14:31:28
  - Maneuver File:
    - Predicted Maneuver Report
  - Maneuver Type:
    - Prograde
    - Orbit Maintenance
    - Maneuver execution error: 2.43%
    - Maneuver pointing error: assumed to be zeros
- A relatively small maneuver error has a big impact on the uncertainty growth rate.

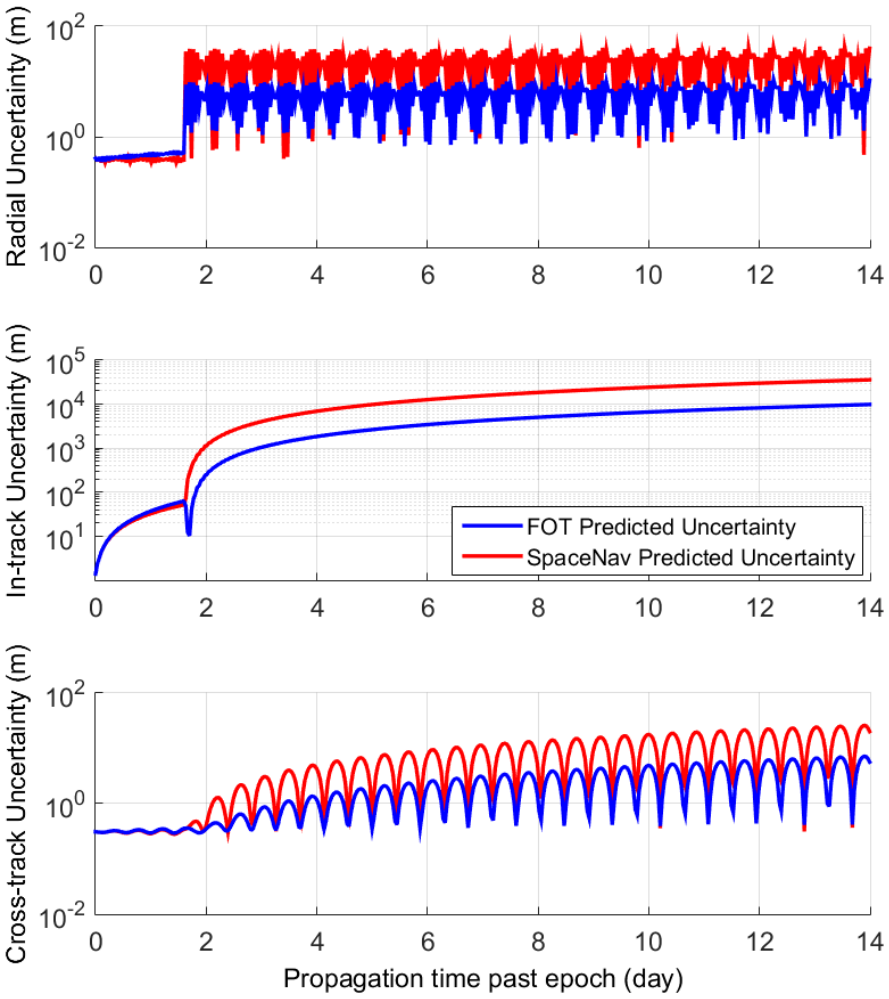

SPACE NAV

Maneuver Uncertainty Implementation
Monte Carlo Validation

Maneuver Monte Carlo Simulation Settings

Sample Size	6,000
Initial State Error	$\sim \mathcal{N}(0, P_0)$, where P_0 = FOT predicted file epoch covariance.
Predicted Maneuver	
Epoch	09/15/17 14:31:28.000 UTC
Type	Posigrade
Magnitude	$\sim \mathcal{N}(0.459, \sigma^2_{\Delta V})$ m/s, where $\sigma_{\Delta V} = 2.43\% \times \lvert\Delta \mathbf{V}\rvert$.

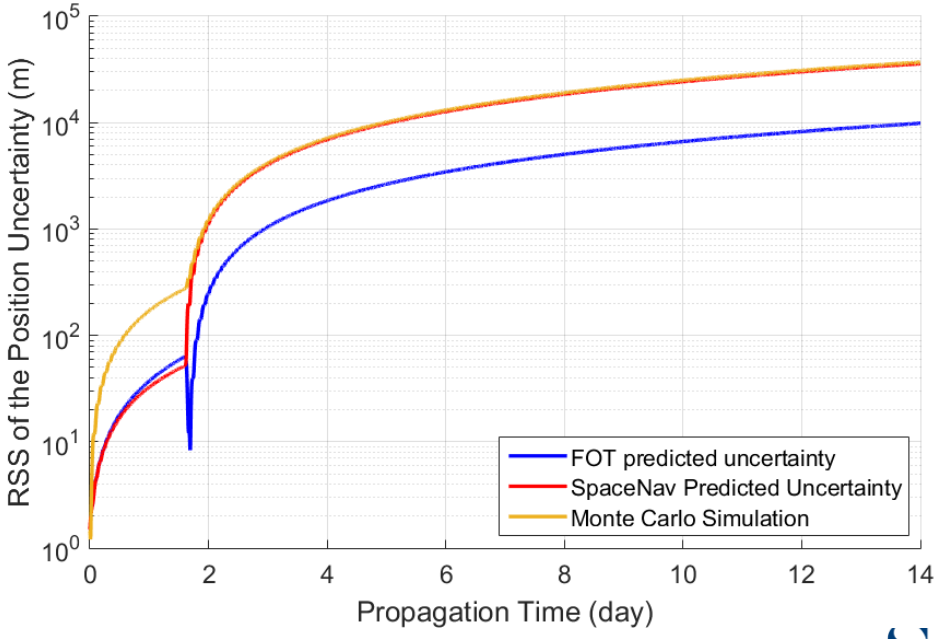

SPACENAV

Conclusion

- A comprehensive analysis of the predicted uncertainty profile of NASA's GPM spacecraft is discussed.
- Analysis of the pass two plus years of GPM definitive and predictive ephemeris files revealed that the propagated uncertainty generated by the GPM flight operations software tends to underestimate the true level of predictive trajectory dispersion, by a significant amount.
- A goodness-of-fit test was carried out to test for the Gaussian distribution hypothesis of the predictive trajectory error population, when those errors are scaled by the GPM provided uncertainty, and when they are scaled by the realistic covariance generated by the SpaceNav covariance realism tool.
- It was shown that the predictive trajectory errors do follow a Gaussian distribution, while the predicted covariance profile provided by the GPM operational software moves the data away from a Gaussian distribution.
- It was further shown that the Gaussian distribution assumption was again valid after the propagated uncertainty profile was corrected via the SpaceNav covariance realism method for specific tuning criteria.
- We further discussed an analysis of the GPM spacecraft past maneuver performance, and the method that is used to incorporate maneuver uncertainty into the propagated realistic covariance.
- This method was validated via a Monte Carlo simulations.
- Results from this study show that scaling the predicted covariance via process noise is a simple and low cost method to produce uncertainty profiles that represent the realistic level of dispersion in the predicted trajectories for SSA applications.

SPACENAV

Acknowledgement

- We would like to thank the GPM flight operations team members for providing the authors with the required data.

- Thanks for your attention!

- Any questions?

- Contact email: Siamak@space-nav.com

SPACENAV

BACKUP SLIDES

An Overview of the GPM Covariance Realism Process Detailed Flowchart

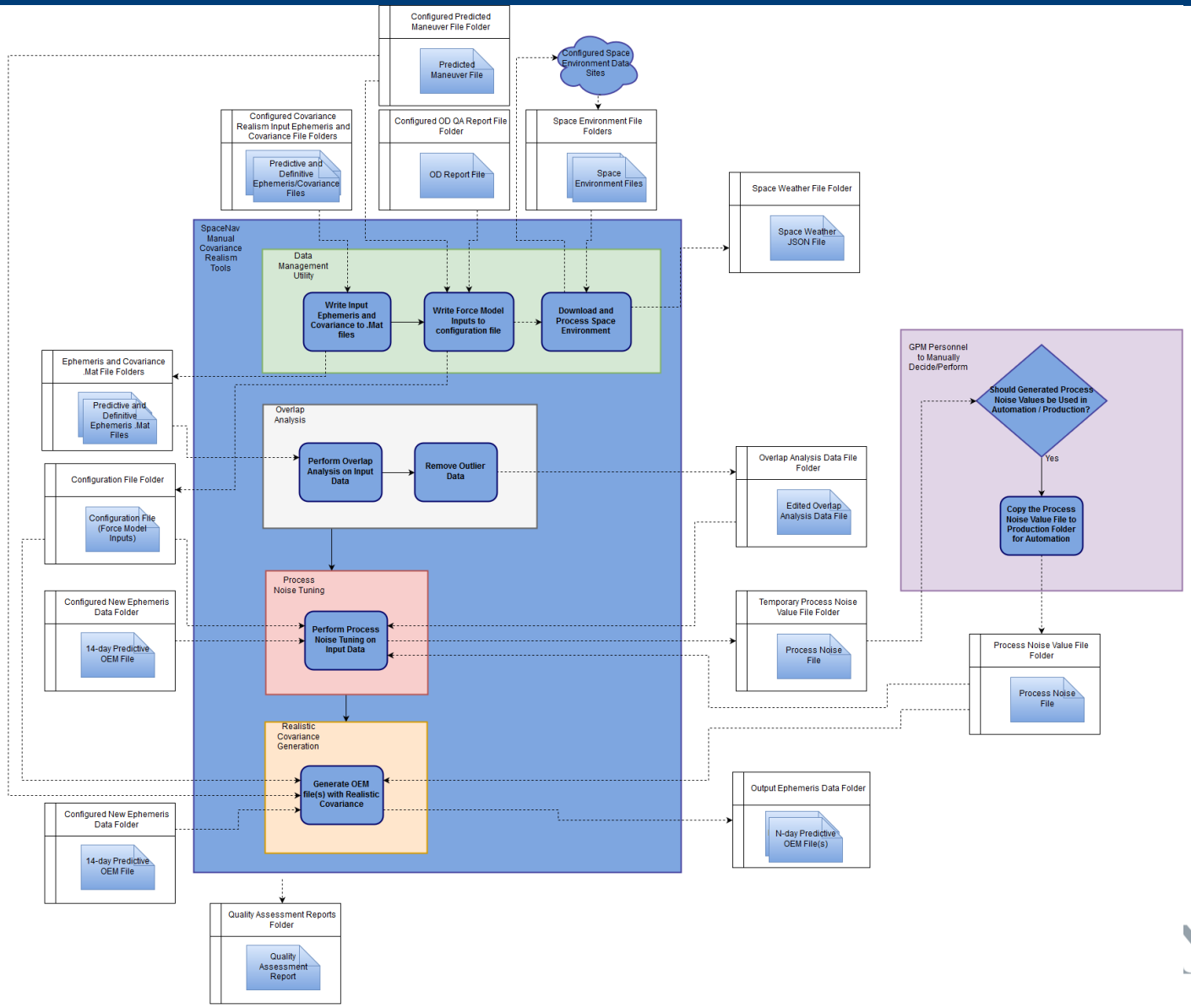

NAV

Chi squared GOF test

- Cramer von Mises (CVM) test statistic
  - Sample population y with empirical cumulative probability distribution function (ECDF) denoted by $F_m(y)$ and hypothesized cumulative distribution function (cdf) $F(y)$

$$\omega^2 = m \int_{-\infty}^{\infty} [F_m(y) - \mathcal{F}(y)]^2 \, dy$$

- Monte Carlo version

$$\omega^2 = \frac{1}{12m} + \sum_{k=1}^{m} \left(\frac{2k-1}{2m} - \mathcal{F}(y_k) \right)^2$$

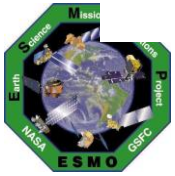

SPACENAV

Process Noise Tuning Optimization Least Squares Solution [1 of 3]

- The process noise tuning process may be optimized by a minimization scheme that aims to minimize the considered metric.
- Let σ_{eph} be the target uncertainty that we wish to achieve
- Therefore, we have $\sigma_{eph} = f(\boldsymbol{\sigma})$ where $\boldsymbol{\sigma}$ is a vector that contains the process noise parameters, i.e.
  - $\boldsymbol{\sigma} = [\sigma_R, \sigma_I, \sigma_c]$
  - $\sigma_R, \sigma_I, \sigma_c$ are the radial, in-track, and cross-track process noise parameters
- The goal of the optimization (tuning) process is to match two uncertainty profiles according to a given metric; The one computed from the ephemeris data (σ_{eph}), and the other that is generated via propagated uncertainty ($\sigma_{prop} = f(\boldsymbol{\sigma}^*)$).

Least Squares Solution [2 of 3]

- Let $\boldsymbol{M}$ is the error metric that we aim to minimize via tuning
- The cost function may be defined by $J = {}^{1}/_{2}\, \boldsymbol{M}^{\boldsymbol{T}} \boldsymbol{M}$
- $\boldsymbol{M}$ is a non-linear function of the tuning set $\boldsymbol{\sigma}^{*}$
- We linearize the error function about the reference tuning set as the following:
  - $\boldsymbol{M} \approx \left.\frac{\partial f(\boldsymbol{\sigma})}{\partial \boldsymbol{\sigma}}\right|_{\boldsymbol{\sigma}^{*}} \delta\boldsymbol{\sigma}$, where $\delta\boldsymbol{\sigma} = (\boldsymbol{\sigma} - \boldsymbol{\sigma}^{*})$
  - Rewrite $\boldsymbol{M} \approx H\delta\boldsymbol{\sigma}$, s.t. $H = \left.\frac{\partial f(\boldsymbol{\sigma})}{\partial \boldsymbol{\sigma}}\right|_{\boldsymbol{\sigma}^{*}}$
- Cost function J is minimized by the least squares solution of the cost function above, i.e.
  - $\delta\boldsymbol{\sigma} = \left(H^{\mathrm{T}} H\right)^{-1} H^{\mathrm{T}} \boldsymbol{M}$

SPACENAV

Least Squares Solution [3 of 3]

- Since we implement a linear solution, one should iterate the solution until convergence
- There are, however, certain caveats for this method
- This method relies on the computation of the derivatives of the cost function at a given point. As a result it would only be applicable to those cases that have a smooth cost function, for which derivatives exist.
- Finally, the linear assumption further relies on the fact that the initial parameter selection is close to the optimal parameter set
- Starting from an initial parameter set that is far from the optimal values, may cause the method to get trapped in local optimum solutions (if any exists, depending on the cost function form)

SPACENAV

Process Noise Optimization Cost Function

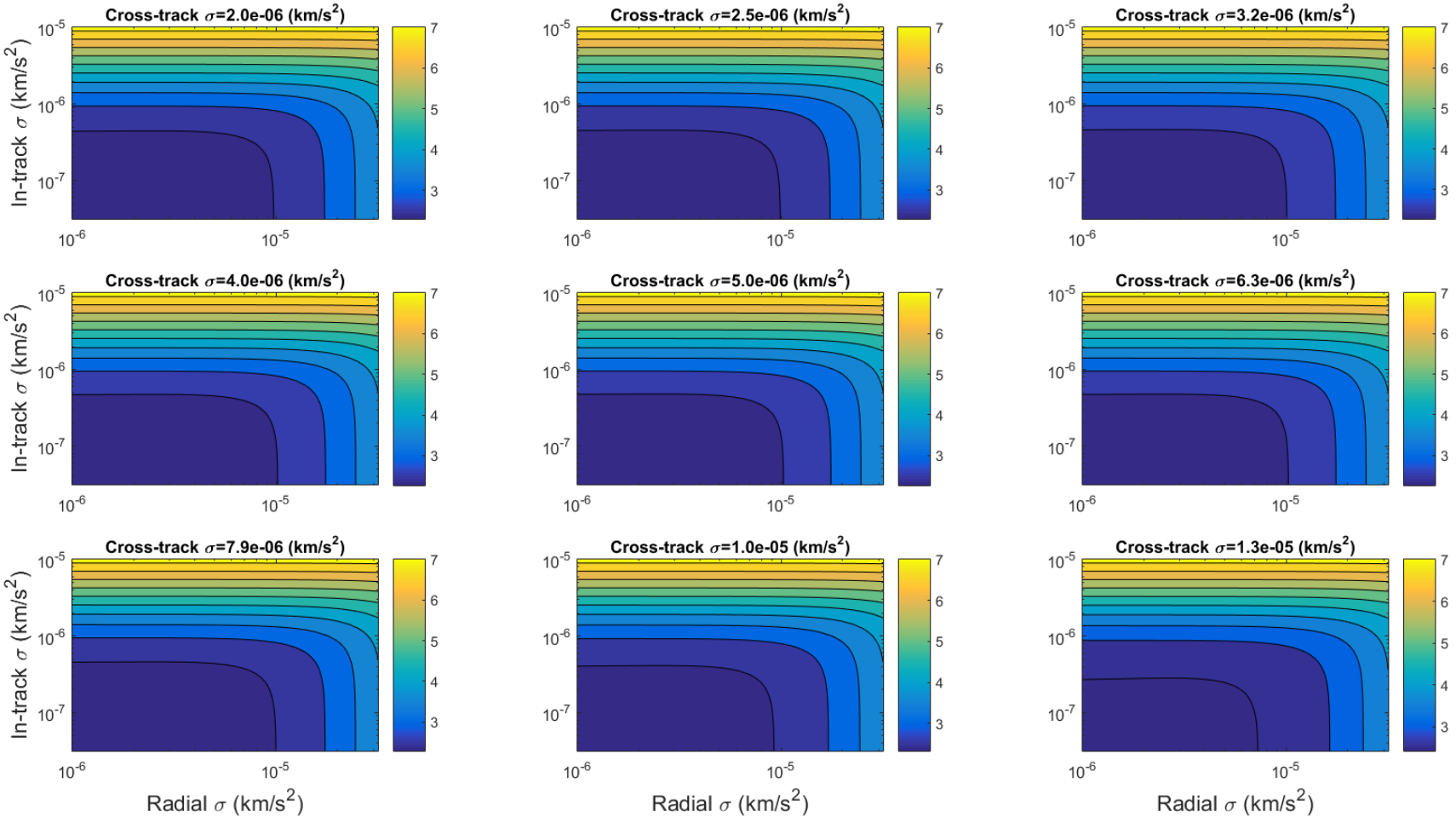

SPACENAV

References

[1] Alfriend, K., and Park, I., "When Does the Uncertainty Become Non-Gaussian," *Advanced Maui Optical and Space Surveillance Technologies Conference*, 2016, p. 46.

[2] Alspach, D., and Sorenson, H., "Nonlinear Bayesian estimation using Gaussian sum approximations," *IEEE Transactions on Automatic Control*, Vol. 17, No. 4, 1972, pp. 439–448. doi:10.1109/TAC.1972.1100034.

[3] Jah, M., and Kelecy, T., "Orbit Determination Performance Improvements for High Area-to-Mass Ratio Space Object Tracking Using an Adaptive Gaussian Mixtures Estimation Algorithm," *60th International Astronautical Congress*, 2009.

[4] Horwood, J. T., and Poore, A. B., "Adaptive Gaussian Sum Filters for Space Surveillance," *IEEE Transactions on Automatic Control*, Vol. 56, No. 8, 2011, pp. 1777–1790. doi:10.1109/TAC.2011.2142610.

[5] Horwood, J. T., and Poore, A. B., "Gauss von Mises Distribution for Improved Uncertainty Realism in Space Situational Awareness," *SIAM/ASA Journal on Uncertainty Quantification*, Vol. 2, No. 1, 2014, pp. 276–304. doi:10.1137/130917296, URL https://doi.org/10.1137/130917296.

[6] Jones, B. A., Doostan, A., and Born, G. H., "Nonlinear Propagation of Orbit Uncertainty Using Non-Intrusive Polynomial Chaos," *Journal of Guidance, Control, and Dynamics*, Vol. 36, No. 2, 2013, pp. 430–444. doi:10.2514/1.57599, URL https://doi.org/10.2514/1.57599.

[7] Foster, J. L., Jr., and Frisbee, J. H., "Comparison of the Exclusion Volume and Probability Threshold Methods for Debris Avoidance for the STS Orbiter and International Space Station," Tech. Rep. NASA/TP-2007-214751, NASA Johnson Space Flight Center, Houston, TX, May 2001.

[8] Foster, J. L., Jr., "The analytic basis for debris avoidance operations for the International Space Station," *Space Debris*, ESA Special Publication, Vol. 473, edited by H. Sawaya-Lacoste, 2001, pp. 441–445.

[9] Chan, F. K., *Spacecraft Collision Probability*, The Aerospace Corporation, El Segundo, CA, 2008. URL https://doi.org/10.2514/4.989186.

[10] Mahalanobis, P. C., "On the generalised distance in statistics," *Proceedings of National Institute of Science, India*, Vol. 2, 1936, pp. 49–55. URL http://ir.isical.ac.in/dspace/handle/1/1268.

SPACENAV

References

[11] Horwood, J. T., Aristoff, J. M., Singh, N., Poore, A. B., and Hejduk, M. D., "Beyond covariance realism: a new metric for uncertainty realism," *Proceedings of the SPIE, Signal and Data Processing of Small Targets, Baltimore, MD*, Vol. 9092, 2014. doi:10.1117/12.2054268, URL https://doi.org/10.1117/12.2054268.

[12] Drummond, O. E., Ogle, T. L., and Waugh, S., "Metrics for evaluating track covariance consistency," *Proceedings of the SPIE*, Vol. 6699, 2007. doi:10.1117/12.740303, URL https://doi.org/10.1117/12.740303.

[13] Stephens, M. A., "Use of the Kolmogorov-Smirnov, Cramer-Von Mises and Related Statistics Without Extensive Tables," *Journal of the Royal Statistical Society. Series B (Methodological)*, Vol. 32, No. 1, 1970, pp. 115–122. URL http://www.jstor.org/stable/2984408.

[14] Tapley, B. D., Schutz, B. E., and Born, G. H., *Statistical Orbit Determination*, Elsevier Academic Press, Burlington, MA, USA, 2004.

[15] Jazwinski, A. H., *Stochastic Processes and Filtering Theory*, Mathematics in Science and Engineering, Vol. 64, Academic Press, Inc., New York, NY 10003, USA, 1970.

[16] Zaidi, W., and Hejduk, M. D., "Earth Observing System Covariance Realism," *AIAA/AAS Astrodynamics Specialist Conference, AIAA SPACE Forum*, 2016. URL https://doi.org/10.2514/6.2016-5628.

[17] Gates, C., *A Simplified Model of Midcourse Maneuver Execution Errors*, JPL technical report, Jet Propulsion Laboratory, California Institute of Technology, 1963. URL https://books.google.com/books?id=YIdTQwAACAAJ.

[18] Wagner, S. V., and Goodson, T. D., "Execution-error modeling and analysis of the Cassini-Huygens spacecraft through 2007," *Proceedings of the AAS/AIAA Space Flight Mechanics Meeting, Galveston, Texas*, 2008.

[19] Wagner, S. V., Arrieta, J., Hahn, Y., Stumpf, P. W., Valerino, P. N., and Wong, M. C., "Cassini Solstice Mission maneuver experience: year three," *Proceedings of the 2013 AAS/AIAA Astrodynamics Specialist Conference, Hilton Head, South Carolina*, 2013.